Assessment of the Possible Uses of Gravity Measurements and Forward Modeling for the Geothermal Projects of Geneva (Switzerland)

Pierrick Altwegg[1], Philippe Renard[2],

[1]MIRARCO, Mining Innovation, Sudbury, ON, Canada
[2]University of Neuchâtel, Center for Hydrogeology and Geothermics, Neuchâtel, Switzerland

Keywords

Geothermal exploration, gravity, forward modeling, deep aquifer, porosity assessment,

ABSTRACT

An important multistage geothermal program led by the Industrial Services of Geneva (SIG) is ongoing in Switzerland. This program named "GEothermie 2020" is aimed at improving the knowledge of the underground of the Swiss-French Greater Geneva Basin to value its geothermal resources. More specifically, the main exploration targets are strike-slip faults affecting Mesozoic series and Kimmeridgian Reef both of which can, locally, show relatively high porosity. In that aim, forward modeling software was used to determine whether and how gravity measurements can be used. This paper summarizes the results of this study and shows that gravity measurements can bring crucial information to the geothermal project especially when exploration targets geometry is well constrained. Indeed in this case it can quantify porosity which can hardly be achieved using other geophysical methods.

1. Introduction

In the region of Geneva (Switzerland), an important multistage geothermal program is ongoing and is led by the Industrial Services of Geneva (SIG). This program named "GEothermie 2020" aims at improving the knowledge of the underground of the Swiss-French Greater Geneva Basin to promote its geothermal resources. One of the objective of the program is to determine which of the existing exploration methods fit the needs of the project with today identified geothermal targets. As the project follows a stepwise approach, the first non-shallow targets are the deep aquifers of the Basin. More specifically, the exploration targets are the strike-slip faults which can be fissure aquifer and karstic aquifer and Kimmeridgian Reef which can, locally, show relatively high porosity.

Those two targets have a common parameter which is a local increase of porosity compared to the rest of the formation. In this respect Altwegg (2015) showed that it is possible to assess porosity of deep aquifer using gravity measurements if enough information of the geothermal reservoir's geometry is available. This paper presents the main results of the study (Altwegg, 2017) that was conducted to assess how this methodology could be used in this purpose.

2. Geology

The Greater Geneva Bassin (GGB) is the westernmost part of the Swiss Mollasse Bassin, a part of the North Alpine Foreland Basin which extend from Savoy to Austria and is linked to the Alpine Orogeny (Homewood et al., 1986; Kuhlemann and Kempf, 2002). GGB itself is limited to the north-west by the Jura Mountains and deepens to the south-east where it is limited by the Salève small range (Figure 1 and 2). Out of the thrust-fold mountain ranges the basin is affected by NW-SE wrench fault system visible on Figure 1. The following brief description of the stratigraphic units mainly refers to Chelle-Michou et al. (2017), Clerc et al. (2015), Rusillon et al. (2016), Sommaruga et al. (2012), Signer and Gorin (1995) and Gorin et al. (1993) in which more detailed information can also be found.

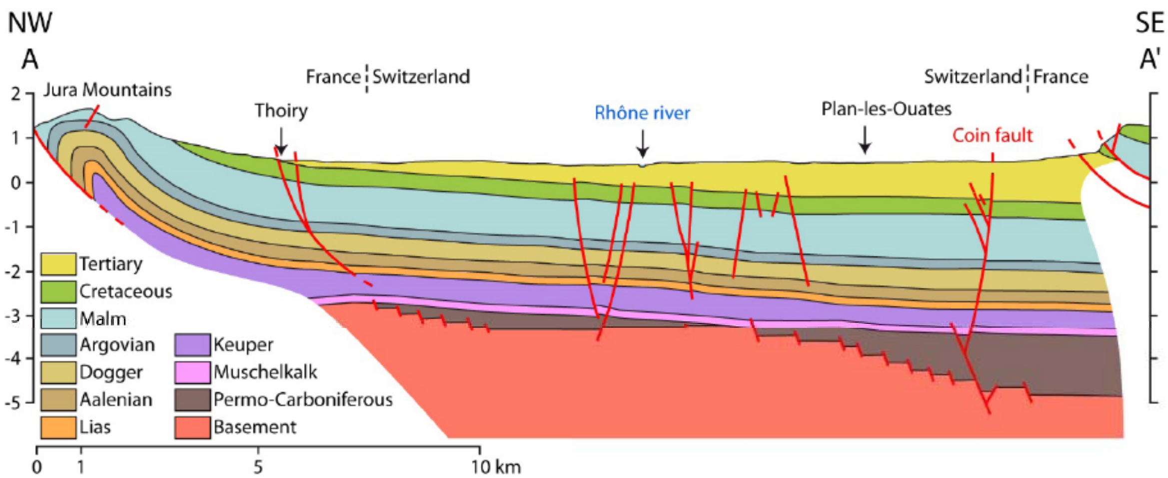

Figure 1: Geological cross-section through the Greater Geneva Basin, quaternary deposits are not shown (modified after Groupe de travail PGG, 2011), localization on Figure 2.

Basement s.l. (encompassing possible Permo-Carboniferous sediments) is covered by sediments composed of Mesozoic and Cenozoic series. Mesozoic series consists mainly in alternating layer of limestone and marls. Upper Malm and Cretaceous are well known for their important thickness of limestone which form the relief of the Jura Mountains. Here to mention that the Kimmerdgian formation (upper Malm) encompass a Reef Complex unit which will be treated in more detail later in this paper as it could show interesting permeability. Moreover, Triassic formation were divided into Muschelkalk and Keuper with this latter encompassing the uppermost of the middle Triassic and the Upper Triassic formations. It was segregated from the rest of the Triassic units as it can show thick sequence of evaporates which can have a dramatic impact on its density.

Cenozoic formations are essentially represented by so-called Molasses deposits essentially consisting of layers of marls and clastic sandstone of Oligocene-Miocene age. Due to the geometry of the basin, the thickness of these deposits considerably vary and can reach 1 – 2 km in deepest part of the GGB. The most recent, unconsolidated deposits are regrouped under the Quaternary layer. In the study area (Figure 2), they are mainly fluvio-lacustrine sediments and can have a relatively important thickness. In this respect and also due their shallow positions and generally low density, these deposits can have a significant impact on gravity measurement.

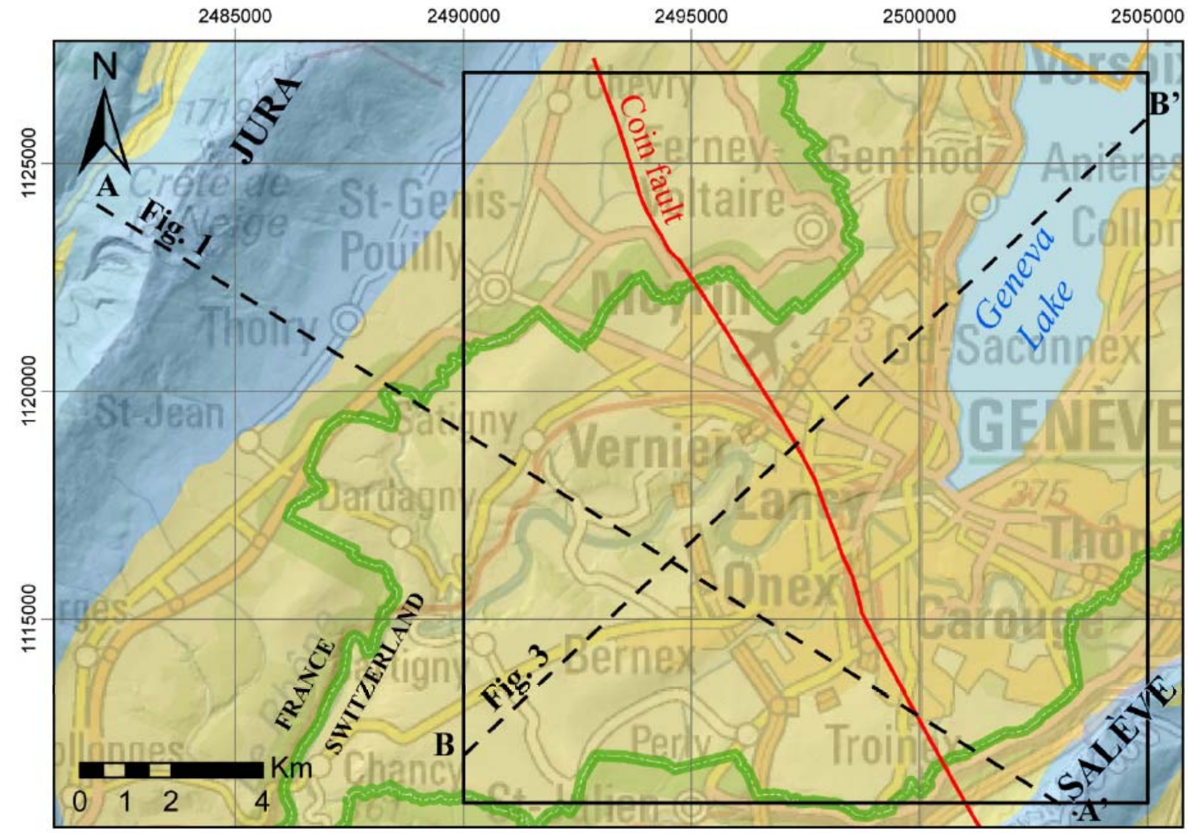

Figure 2: Regional tectonic map and extent of the study area (black rectangle). Dashed lines: trace of geological cross sections, red line: Coin fault trace, Light blue area: Mesozoic Formation of the Jura and Salève range, Yellow area: Cenozoic molasses, coordinates system is CH1903+.

From a geothermal point of view, the Permo-Carboniferous, Muschelkalk, Dogger, Upper Malm and Cretaceous formations shows interesting reservoir properties. This is especially true when these formation shows a reef facies and/or are affected by a fault which can locally increase permeability and allows for increased karstification. However even if it shows interesting reservoir properties and was drilled by the Humilly-2 borehole (Marti, 1969) a few kilometer south-west of the study area, Permo-Carboniferous deposits are not considered as a potential geothermal target for the current projects. This is mainly due to present day sparse information available especially regarding the geometry of the graben.

3. Material and methods

As mentioned in the introduction, the aim of this study is to evaluate how gravity measurement can help with the exploration of geothermal targets of the GEothermie 2020 project. Presently, those targets are the strike-slip fault affecting Mesozoic formations and the Kimmeridgian reef. In addition, the effect of Quaternary deposits was also evaluated as it can hinder the detection of geothermal targets gravity effect (not shown in this paper). This study main goal is thus to establish the driving parameters allowing the detection of the geothermal targets using gravity measurements. However, an evaluation of the effect on gravity of the seismic data uncertainty on depth was also conducted.

Several goals of this study are to determine whether a structure can be detected by gravity measurements or not and therefore we need to set a detection limit. According to Olivier et al. (2010), uncertainty on available gravity data is around 0.3 mGal but Altwegg (2015) as well as Mauri et al. (2017, 2015) showed that using more recent data treatment allows to decreases this value under 0.1 mGal. In this respect, in this study, we considered the value of 0.1 mGal as an absolute lower detection limit and 0.3 mGal as the upper detection limit.

To achieve the different goals of this study we used GInGER (GravImetry for Geothermal ExploRation) software (Altwegg, 2015; Altwegg et al., 2015a) which allows to compute the gravity effect of 3D geological model and was specially designed to assess porosity of fault zones. Here to mention that, in most modeling software, faults are represented using planes but as a plane has no volume it also doesn't have any gravity effect. That's the reason why, GInGER considers faults damages zones i.e. the volume of rock affected by the fault in the gravity model.

The software convert all the geological structures present in the 3D geological model into prism and uses the algorithm from Blakely (1996) to compute their effect on gravity. More detailed information on the methodology, software as well as two case studies can be found in Altwegg (2015). Eventually, this software allows to compare computed to measured gravity and to adapt the density of the different elements in real time. Therefore, in order to establish the gravity effect of different parameters of geological structures, we analyzed the difference (or misfit) between a modified and a reference model which is presented in the next point.

3.1. Gravity model

Apart of the topography and the base of Quaternary deposits, a geological model is used to generate the gravity model. In this study this model, is a portion of the one established by N. Clerc during his PhD (in prep.) which is also part of the GEothermie 2020 project. It is composed of 11 geological limits modified after the GeoMol (2015) model.

In order to establish the reference (gravity) model, we first evaluated the impact on the gravity response for two different reference density and of the fusion of different layers in the model. Indeed, the majority of gravity measurements collected in the field are relative measurements, meaning that they are compared to an idealized model of the earth which has a density. This density used to compute the Bouguer Anomaly is of critical importance as it will increase or decrease the relative effect of geological structure depending on their own density. In our case, we tested two densities to determine which was the best suited for our target. Those two densities, used by the Swiss Atlas of Gravity (Olivier et al., 2010) are 2550 and 2670 $kg \cdot m^{-3}$ and represents the average density of the Molasses sediments and of the upper crust respectively. In this respect, we computed the effect of each layer present in the geological model for the density values of Table 1 and for those two reference densities. This allowed us to determine range for gravity effect of each layer and compare them to each other.

Table 1: Geological model layer density range in kg·m^{-3} used in this study (adapted from Altwegg, 2015 and references herein). 1. Value used for Keuper and Liassic as is may contain evaporites.

Layer	Minimum		Admitted	Maximum	
	Literature	Local		Local	Literature
Quaternary	700	2000	2170	2350	2600
Molasse	1800	2450	2550	2700	3200
Mesozoic	1800	2550 (2300)[1]	2680	2700	2900
Basement s.l.	2500	2600	2670	2750	3000

The following remarks are made for the case considered closest to reality, i.e. when the layer density are set to the value of the grayed column of Table 1. Values in this table are from literature (Altwegg, 2015 and references herein) and ranges were corrected to better reflect variation expected in the study area. For these values, we observed that with a reference density of 2670 kg·m^{-3}, the effect of the Molasse and Quaternary layer represent 80% of the effect of the model, basement s.l. has no effect and Mesozoic layers only have a light effect if Keuper is not considered. On the contrary, when the reference density is set to 2550 kg·m^{-3} the part of the effect of the Molasse and Quaternary layers on the overall response of the model are reduced as well as the one from Keuper. This implies that the gravity effects of the Mezosoic layers are highlighted but also that the basement count for almost 40% of the effect of the model.

Due to their small thickness, layers of the Cretaceous, Lower Malm and Muschelkalk don't have an important gravity effect and this latter is also quite constant on the whole study area. However, as those small layers hinder results of density inversion, we wanted to quantify how merging them with another layer will impact the overall model gravity response. In this respect, we merged Cretaceous to Upper Malm as well as Lower Malm to Dogger. As their assumed densities are the same to the layer with which they are merged, no difference to the overall gravity effect of the model is induced. Concerning Muschelkalk layer, from a gravity point of view, it can be merged with Keuper or Basement s.l. However, even if its assumed density is closer to the one of the Basement s.l. it was merged to the Keuper layer as their geometry are closer and are both composed of sediments. Following this action we minimized the misfit to the previous model by running inversion on the density of the Keuper and basement. Result shows that changing those layers density by as few as 5 kg·m^{-3} was enough to reduce the maximum misfit over the most part of the study under 0.15 mGal which is close to lowest detection limit considered in this study.

As previously mentioned, one of the main goal of this study is to establish the gravity effect of a fault zone. In this respect, a simplified (vertical) model of the Coin fault (Figure 1 and 2) which crosses the whole basin and is the best constrained fault-zone in GGB, was added to the reference model. For each fault parameter studied, the effect of the model is re-computed after its value was modified and the obtained result is compared to this reference model. This model has the following parameters: geological layers densities are set to the value of the grayed column of Table 1. The reference density is 2550 kg·m^{-3}, fault is vertical extend from the bottom of the Mesozoic to half of the molasses layer. Its damage zone has a width of 200 m and induce a decrease of density of 5%. The Gravity effect of this model on the BB' profile (localization on Figure 2) is shown on Figure 3.

4. Results

One of the targets of this study is to evaluate the often neglected gravity effect induced by uncertainty on 3D geological models' layers geometry. As it is mainly based on 2D seismic data, uncertainties are mainly linked to data density and time-depth conversion. However, we limited this study to the latter one. Quantification of this effect was done by changing the depth of the top Mesozoic, top Keuper and base Mezosoic limits independently. These limits were selected because of the density contrast existing between the two layers they separated. To better illustrate the kind of uncertainties that can occur, two methods were used to change the depth of the layer. The first is a translation of the limit of 50 m for the Top Mesozoic, 100 m for top Keuper and 250 m for base Mesozoic. Those value were set to reflect the increase of uncertainties with depth and the absorption of the seismic energy in the evaporites. The second methods consist in applying a factor to depth. The value of 5 and 10% were selected the first one being the accepted value for uncertainties for depth for the Sankt Gallen 3D seismic survey in the eastern part of the Swiss Molasse Basin (Altwegg et al., 2015b).

In each case, the effect of the model is re-computed after modification of the limit and its effect compared to the original (reference) model. Results showed density variation of up to 0.5 mGal which is higher than the assumed maximum detection limit. However, running inversion on the densities, we were able to reduce this variation to under 0.05 mGal. This is a good illustration of the equivalence principle (e.g. Griffiths and King, 1981) applicable on the potential methods i.e. that no unique solution exists that allows the determination of the depth/geometry and density of the layers.

4.1. Gravity effect of fault zone

The software allows us to separate the effect of each fault compartment, i.e. the gravity effect of each rock volumes affected by the fault for each geological layer. Using this feature, we were able to determine that even if the maximum intensity of the fault is induced by the Molasse part, it is the Mesozoic part of the fault which will allows its detection as it induces an anomaly of smaller intensity but of longer wavelength. We were also able to determine that it was not possible to detect if the fault continues into the basement using gravity measurements. Indeed, the anomaly induced by a fault of 1000 m in the upper part of the basement only induce a maximum anomaly of less than 0.1 mGal which is under the detection limit.

The main target of the study is to determine the gravity effect of a change of density induced by the fault. This change of density is considered to be induced by the open fracture present in the damage zone. We therefore aimed at quantifying this gravity effect when those fracture are filled with air as well as water. Results, presented on Figure 3 on the BB' profile, showed that a minimum reduction of 3% of the layers bulk density was sufficient to be detectable and that this value raise to 5% if the fracture is saturated. Moreover, using these results, we were able to determine the average distance at which the lower (0.1 mGal) and upper (0.3 mGal) detection limit were located (Figure 3, lower right).

Depth of top Mesozoic was suspected to be a prominent parameter regarding the gravity effect of fault. However results showed that it mainly impact the maximum intensity of the anomaly induced by the structure. This means that, for the GGB, it doesn't seems to significantly influence the detection possibilities a fault zone using gravity measurements.

Regarding fault zone, the last considered parameter was the width of the damage (or fractured) zone. In this respect, three models with different width (100, 200 and 500 m) as well as a fourth model with a flower structure were considered. Results showed that this parameter has a major impact on the intensity of the anomaly as it increase the considered volume. However, using the same four models, we were able to reproduce the effect of the reference model fault (width of 100 m, Figure 3, 5% black line) with different densities. This shows us that using gravity measurement, it is only possible to assess porosity if the geometry of the fault damage zone (or reservoir) is well constrained by other methods such as 3D seismic data.

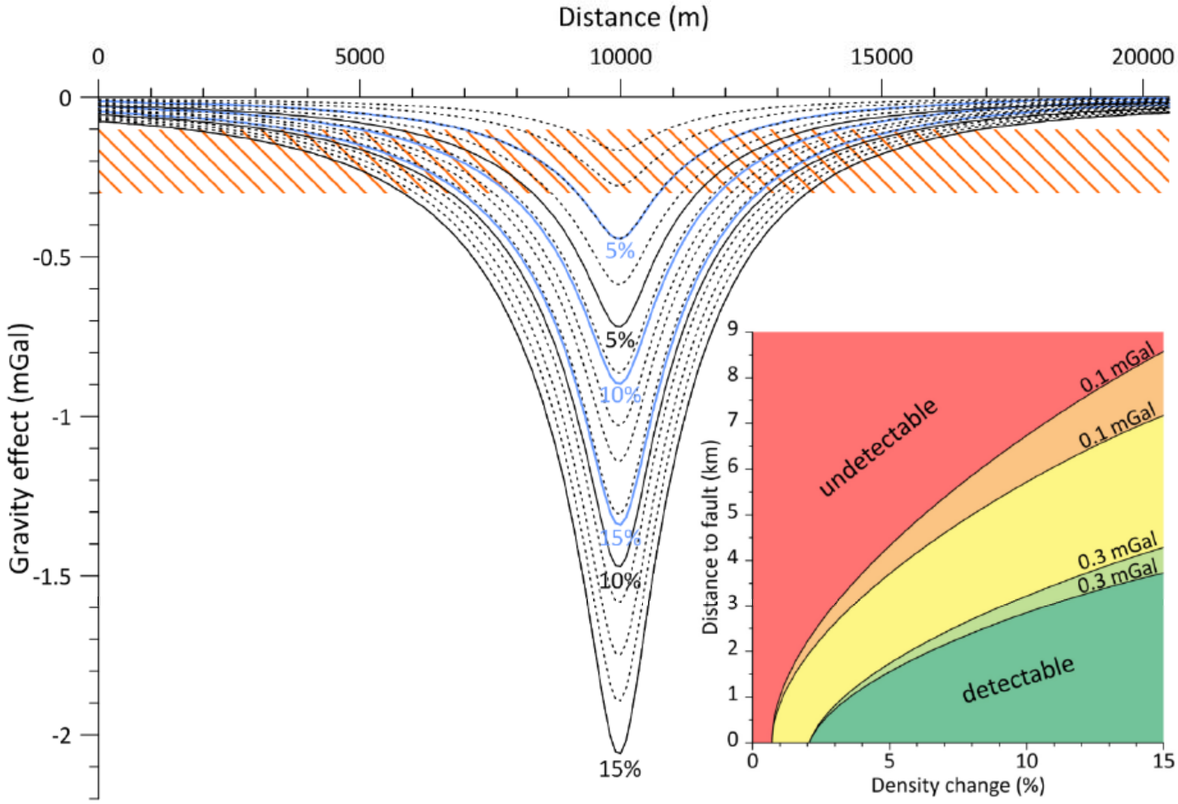

Figure 3: Gravity effect and detection limit (lower right) of a density reduction induced by the fault zone on the BB' profile (Figure 2). Blue lines represent this effect when those volume are saturated. Hatched zone symbolize the upper and lower limit of detection which were plotted vs distance in the lower right plot (see text for more details). Fault medium plane is located at 9975 m from profile start.

4.2. Gravity effect of Kimmeridgian Reef

Other potential geothermal targets are Kimmeridgian reefs as they can show, locally, higher porosity compared to the rest of the Malm. By analogy with fault zones, this localized change of porosity should induce a change of density that could potentially be detected using gravity measurements. We first conducted a preliminary study that showed that those structure are likely detectable but also that we are close to the detection limit (Figure 4). In that case, a map of possible location of the reef (Figure 4A) as well as a top and bottom seismic horizon (Figure 4B) allowed us to determine the geometry. The gravity effect of the structures were then computed using a density of 2160 $kg{\cdot}m^{-3}$. This density represent a reduction of 20% compared to the average Malm density (Table 1) which is the maximum porosity value considered for these structures according to Rusillon et al. (2016). However, as the localization as well as the extension of these structures in the GGB is highly uncertain, we increased their x, y dimensions by 100 m and re-computed their gravity effect to take that into account. The gravity effect of this change, visible on (Figure 4A, red lines), show an important increase of effect making more likely detectable.

Due to this results, we a parametric study was performed to establish the influence of depth, density and dimensions of the structures on their induced gravity effect and thus to our capacity to detect them using gravity measurements. For this purpose, reefs were modeled by a single prism. Again individual parameters are studied independently and compare to a reference model. In this case, this model is a square prism which base is located at 100 m with side dimension of 1500 m and a thickness of 125 m. This volume is considered to have a density difference with the rest of the geological formation of 270 $kg{\cdot}m^{-3}$. In this case we didn't use GInGER but another software that computes the gravity effect of a single prism based the same algorithm (Blakely, 1996).

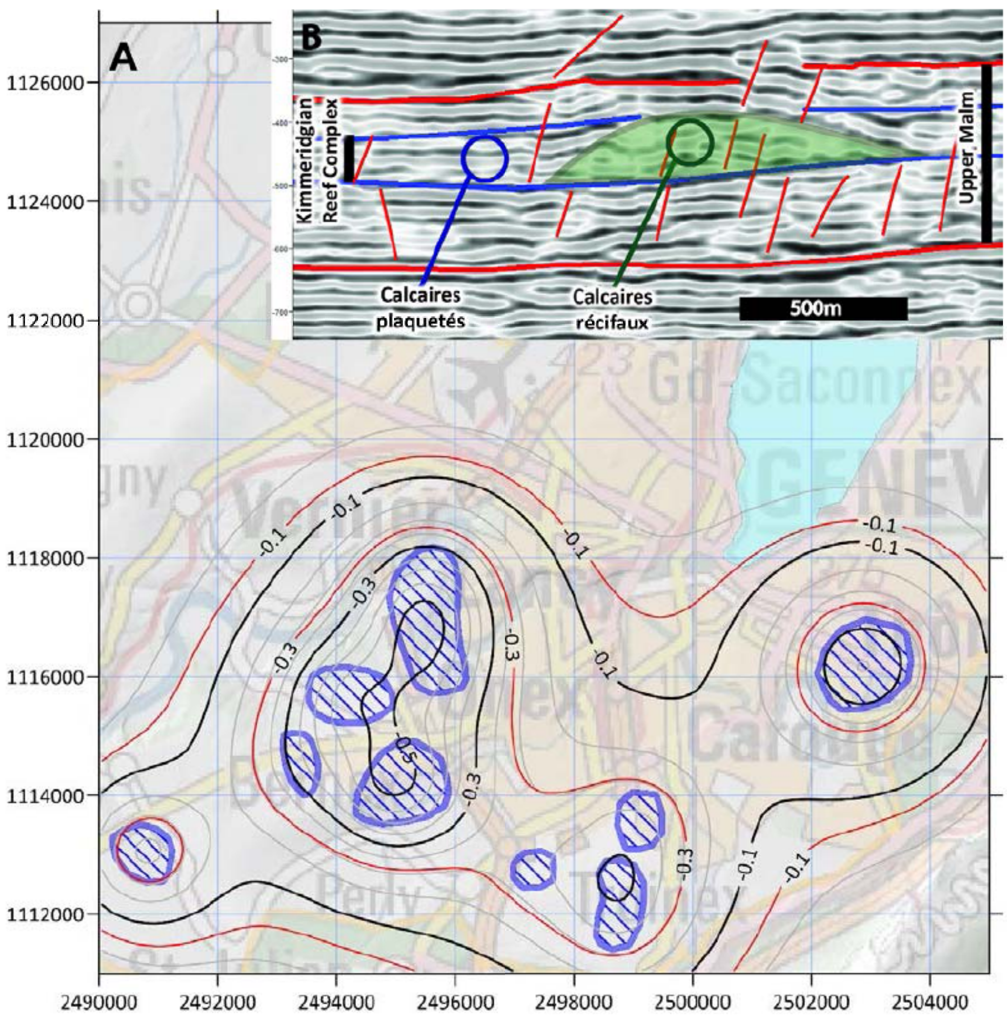

Figure 4: A. Gravity effect (in mGal) induced by possible Kimmeridgian Reefs (black lines) localized by 2D seismic data (hatched shape, Clerc, pers. Com). Those shape were extended horizontally by 100 m (blue area) and their gravity effect recomputed (red lines). Coordinates system is CH1903+. B. Example of 2D seismic showing a Kimmeridgian Reef Complex (Rusillon et al., 2016).

An example of result archived by this study in which one of the prism's base side dimension was modified, is shown on Figure 5. Globally, the parametric study showed that there are no prominent parameters (within the considered range) and that structure needed to have at least a base side dimension (square) of 1500 m, a thickness of 125 m, and a density reduction of 540 kg·m^{-3} (10% compare to the rest of the formation) to be detectable by gravity measurements.

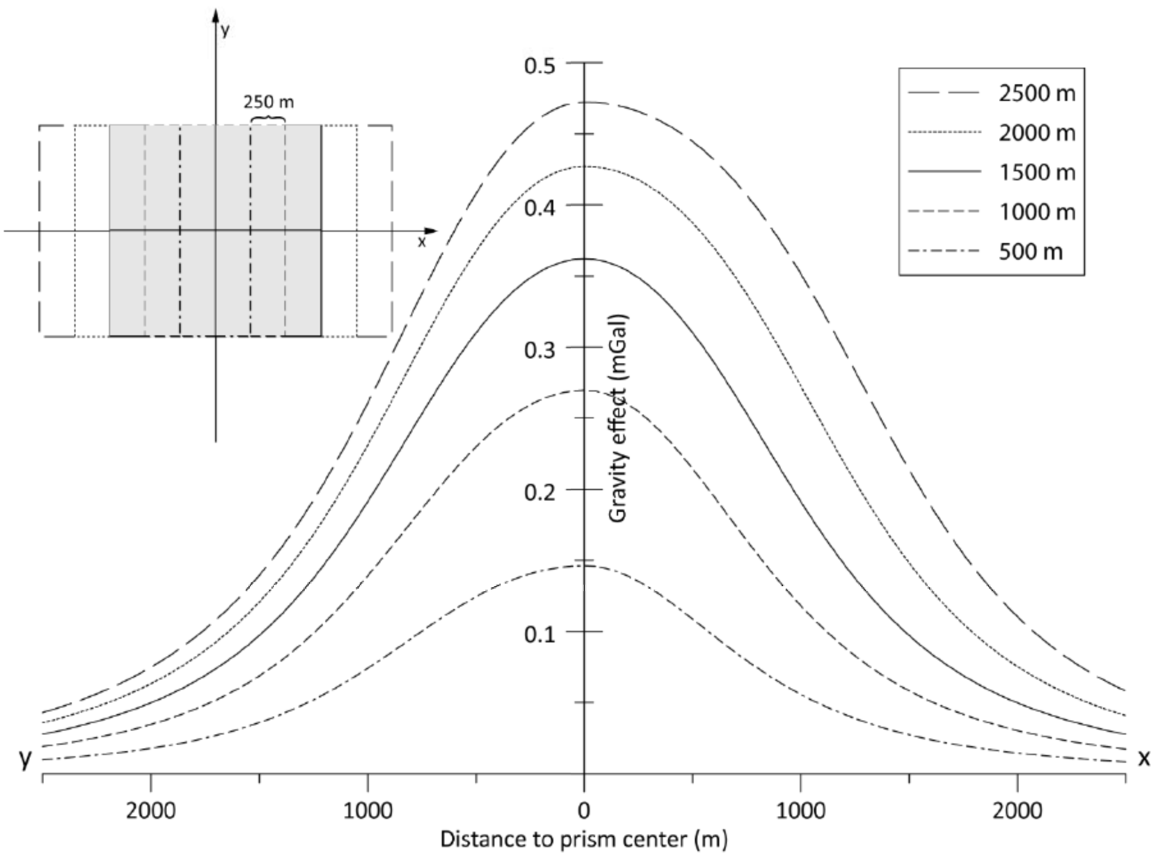

Figure 5: Gravity effect induced by a change of length of one of the prism's side in two perpendicular directions. Other parameters of the prism which is used to model Kimmeridgian Reefs are kept constant: thickness 125 m, depth of base 1000 m, difference of density 270 kg·m^{-3}. This effect on the is shown on the right of the y axis for the x direction and on the left of the y axis for the y direction as symbolized on the upper left sketch)

These values are close to the maximum values considered for the parameters of the considered structures which were base on present day knowledge on them. However as previously mentioned, information on those structures is scarce particularly data related to their extension and localization. Therefore, and as long as no new data has been collected, it seems unlikely that these structures can be detected using gravity measurement alone in the GGB. Nevertheless, if this effect is superposed to the one of a fault zone like the one studied in this paper, it should increase the odds.

5. Conclusions

Forward modeling on gravity effect of a 3D model using GInGER allowed for quantifying the gravity effect of the considered geothermal targets for the GEothermie 2020 project. This study shows that while gravity can be used to assess induced porosity of a fault zone given the geological setting of the project, it is only possible if the geometry of the reservoir is well known. This study also shows that it may be possible to detect reef structure for depth around 1000 m. However, due to high uncertainty of the localization, geometry and density of these structures this result is to be considered with caution and new data should be collected to confirm it. Results of this study clearly show that gravity measurements can bring crucial information to geothermal project such as assessing porosity and help in determining the targets as well as the geometry of a survey.

REFERENCES

Altwegg, P., 2017. Possibilités d'utilisation de la gravimétrie dans le cadre du projet géothermie 2020 de SIG - Rapport final (No. MRM002-00112). MIRARCO, Sudbury, Ontario, Canada.

Altwegg, P., 2015. Gravimetry for geothermal exploration (PhD Thesis). Université de Neuchâtel.

Altwegg, P., Renard, P., Schill, E., Radogna, P.-V., 2015a. GInGER (GravImetry for Geothermal ExploRation): A New Tool for Geothermal Exploration Using Gravity and 3D Modelling Software, in: Proc. World Geothermal Congress 2015. Melbourne, Australia, p. 7.

Altwegg, P., Schill, E., Abdelfettah, Y., Radogna, P.-V., Mauri, G., 2015b. Toward fracture porosity assessment by gravity forward modeling for geothermal exploration (Sankt Gallen, Switzerland). Geothermics 57, 26–38. doi:10.1016/j.geothermics.2015.05.006

Blakely, R.J., 1996. Potential theory in gravity and magnetic applications. Cambridge University Press.

Chelle-Michou, C., Do Couto, D., Moscariello, A., Renard, P., Rusillon, E., 2017. Geothermal state of the deep Western Alpine Molasse Basin, France-Switzerland. Geothermics 67, 48–65. doi:10.1016/j.geothermics.2017.01.004

Clerc, N., Rusillon, E., Moscariello, A., Renard, P., Paolacci, S., Meyer, M., 2015. Detailed Structural and Reservoir Rock Typing Characterisation of the Greater Geneva Basin, Switzerland for Geothermal Resource Assessment, in: Proc. World Geothermal Congress 2015. Melbourne, Australia, p. 10.

GeoMol, T., 2015. GeoMol—assessing subsurface potentials of the Alpine Foreland Basins for sustainable planning and use of natural resources—Project Report. Augsbg. Bavar. Environ. Agency.

Gorin, G.E., Signer, C., Amberger, G., 1993. Structural configuration of the western Swiss Molasse Basin as defined by reflection seismic data. Eclogae Geol. Helveticae 86, 693–716.

Griffiths, D.H., King, R.F., 1981. Applied geophysics for geologists and engineers: the elements of geophysical prospecting. Pergamon press Oxford.

Groupe de travail PGG, 2011. Evaluation du potentiel géothermique du canton de Genève (PGG) Vol.1 : Rapport final, Vol.2 : Annexes (No. 5753/1). GADZ, Genève.

Homewood, P., Allen, P.A., Williams, G.D., 1986. Dynamics of the Molasse Basin of western Switzerland. Foreland Basins Ed PA Allen P Homewood Int Assoc Sediment Spec 8, 199–217.

Kuhlemann, J., Kempf, O., 2002. Post-Eocene evolution of the North Alpine Foreland Basin and its response to Alpine tectonics. Sediment. Geol. 152, 45–78.

Marti, J., 1969. Rapport de fin de sondage d'Humilly 2. SNPA, direction exploration et production, division Europe. Rapport 33 p., annexes 99p.

Mauri, G., Marguet, L., Jansen, G., Marti, U., Baumberger, R., Allenbach, R., Kuhn, P., Altwegg, P., Miller, S.A., 2017. Combine used of land gravity data and 3D geological model to image deep geological basin: Case of Region of La Broye, Switzerland. Presented at the IASTEM 136th International Conference on Environment and Natural Sciences (ICENS), Seoul, South Korea.

Mauri, G., Marguet, L., Jansen, G., Olivier, R., Marti, U., Baumberger, R., Allenbach, R., Kuhn, P., Altwegg, P., Miller, S.A., 2015. Gravity prospection in region of La Broye. Presented at the 13th Swiss Geoscience Meeting, Basel, Switzerland.

Olivier, R., Dumont, B., Klingelé, E., 2010. L'Atlas gravimétrique de la Suissse. Géophysique 43.

Rusillon, E., Clerc, N., Brentini, M., Moscariello, A., 2016. Rock typing, structural characterization and stratigraphy harmonization in support of geothermal exploration in the Greater Geneva Basin (Switzerland), in: Proceedings. Presented at the European Geothermal Congress 2016, Strasbourg, France, p. 10.

Signer, C., Gorin, G.E., 1995. New geological observations between the Jura and the Alps in the Geneva area, as derived from reflection seismic data. Eclogae Geol. Helvetiae 88, 235–265.

Sommaruga, A., Eichenberger, U., Marillier, F., Kissling, E., 2012. Seismic Atlas of the Swiss Molasse Basin, Matér. Géol. Suisse, Géophysique. Swiss Geophysical Commission.